

ANTIBACTERIAL AND ANTICANCER STUDIES OF MONONUCLEAR AND BINUCLEAR COMPLEXES OF TELLURIUM(IV), TANTALUM(V), SELENIUM(IV), AND NIOBIUM(V) URATE BY SPECTROSCOPIC METHODS

F. A. Al-Saif¹, J. Y. Al-Humaidi¹, D. N. Binjawhar¹,
H. A. Bakhsh¹, M. S. Refat^{2,3*}

¹ Department of Chemistry, College of Science at Princess Nourah bint Abdulrahman University, Riyadh 11671, Saudi Arabia

² Department of Chemistry, College of Science at Taif University, Al-Haweiah, Zip Code 21974, Taif, Saudi Arabia

³ Department of Chemistry at Port Said University, Port Said, Egypt; e-mail: msrefat@yahoo.com

Novel tellurium(IV), tantalum(V), selenium(IV), and niobium(V) urate complexes were prepared with molar ratios 1:1 and 2:1 (metal:ligand). The uric acid (H_4UA) ligand was reacted with $TeCl_4$, $TaCl_5$, $SeCl_4$, and $NbCl_5$ metal chlorides in the presence of NaOH to yield mononuclear and binuclear complexes. The mononuclear tellurium (IV) and tantalum(V) complexes formulas $[Te(H_3UA)(H_2O)_3(Cl)] \cdot 2Cl \cdot 2H_2O$ (I) and $[Ta(H_3UA)(H_2O)_2(Cl)_2] \cdot 2Cl \cdot 4H_2O$ (II), as well as binuclear selenium(IV) and niobium(V) complexes $[Se_2(H_2UA)(Cl)_4] \cdot 2Cl \cdot 4H_2O$ (III) and $[Nb_2(H_2UA)(Cl)_8] \cdot 3H_2O$ (IV), were obtained in the presence of NaOH at pH 8–9. The metal complexes were characterized by elemental analyses, FTIR, ¹H-NMR, electronic, conductivity, and thermal analyses. In the case of mononuclear complexes, the coordinating sites are the pyrimidine carbonyl oxygen atom of C(6)=O group and imidazole nitrogen of deprotonated N(7)–H. In addition to these coordinating sites, the pyrimidine carbonyl oxygen atom of C(2)=O and pyrimidine nitrogen of deprotonated N(3)–H are involved in coordination in binuclear complexes. The metal urate complexes exhibited six-coordinate geometries, while the binuclear selenium is four-coordinate. The antibacterial and anticancer activities of the urate complexes were investigated. No antibacterial activity was observed in any treatments, except for gram-negative *Klebsiella*, which showed a slight effect. The metal complexes showed high proportions of cell viability percentage after treatment in both colorectal adenocarcinoma (Caco-2) and breast cancer (MCF-7) cell lines using the neutral red uptake assay.

Keywords: urate, Te^{4+} , Ta^{5+} , Se^{4+} , Nb^{5+} , coordination, spectroscopy, antimicrobial activity.

ИССЛЕДОВАНИЕ АНТИБАКТЕРИАЛЬНОЙ И ПРОТИВООПУХОЛЕВОЙ АКТИВНОСТИ МОНОНУКЛЕАРНЫХ И БИЯДЕРНЫХ КОМПЛЕКСОВ УРАТОВ ТЕЛЛУРА(IV), ТАНТАЛА(V), СЕЛЕНА(IV) И НИОБИЯ(V) СПЕКТРОСКОПИЧЕСКИМИ МЕТОДАМИ

F. A. Al-Saif¹, J. Y. Al-Humaidi¹, D. N. Binjawhar¹,
H. A. Bakhsh¹, M. S. Refat^{2,3*}

УДК 543.42:576.8.06

¹ Научный колледж Университета принцессы Нуры бинт Абдулрахман, Эр-Рияд 11671, Саудовская Аравия

² Научный колледж Таифского университета, Аль-Хавейя, 21974, Таиф, Саудовская Аравия

³ Университет Порт-Сауда, Порт-Сауд, Египет; e-mail: msrefat@yahoo.com

(Поступила 17 февраля 2020)

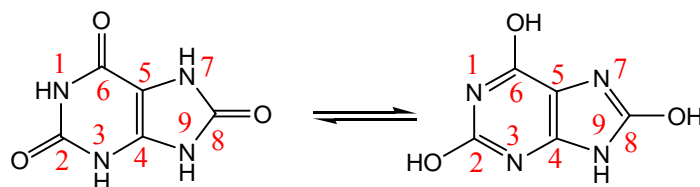
Получены уратные комплексы теллура(IV), тантала(V), селена(IV) и ниобия(V) в молярном соотношении металл:лиганд 1:1 и 2:1. Моноядерные и биядерные комплексы получены реакцией лиганда мочевой кислоты (H_4UA) с хлоридами металлов $TeCl_4$, $TaCl_5$, $SeCl_4$ и $NbCl_5$ в присутствии

NaOH. Моноядерные комплексы теллура(IV) и тантала(V) $[Te(H_3UA)(H_2O)_3(Cl)] \cdot 2Cl \cdot 2H_2O$ (I) и $[Ta(H_3UA)(H_2O)_2(Cl)_2] \cdot 2Cl \cdot 4H_2O$ (II), а также биядерные комплексы селена(IV) и ниобия(V) $[Se_2(H_2UA)(Cl)_4] \cdot 2Cl \cdot 4H_2O$ (III) и $[Nb_2(H_2UA)(Cl)_8] \cdot 3H_2O$ (IV) получены в присутствии NaOH при pH 8–9. Комплексы охарактеризованы методами ИК-Фурье- и 1H ЯМР-спектроскопии, а также элементного, электронного, термического анализа и анализа проводимости. В случае моноядерных комплексов координационными центрами являются атом кислорода пиридинкарбонильной группы C(6)=O и имидазольный азот депротонированного N(7)–H. Помимо этих координационных центров пиридинкарбонильный атом кислорода C(2)=O и азот пиридина депротонированного N(3)–H участвуют в координации в биядерных комплексах. Уратные комплексы металлов имеют шестикордонатную геометрию, биядерный селен — четырехкоординатную. Исследована антибактериальная и противоопухолевая активность уратных комплексов. Антибактериальная активность не наблюдалась, за исключением активности граммотрицательной клебсиеллы. Показана высокая жизнеспособность клеток после лечения в клеточных линиях колоректальной аденокарциномы (Caco-2) и рака груди (MCF-7) с использованием анализа поглощения нейтрального красного.

Ключевые слова: урат, Te^{4+} , Ta^{5+} , Se^{4+} , Nb^{5+} , координация, спектроскопия, антимикробная активность.

Introduction. Uric acid (H_4UA) in serum is the final product of the metabolism of purine nucleotides, and overproduction or decreased kidney secretion of uric acid leads to hyperuricemia in humans [1, 2]. The prevalence of hyperuricemia in the general population is estimated to be 10–25%. High blood uric acid concentration can lead to gout; **gout is** associated with many medical conditions, including metabolic syndrome, cardiovascular disease, diabetes, and renal impairment [1]. In epidemiology studies, uric acid in the blood has been identified as a risk factor for high blood pressure, dyslipidemia, and cardiovascular and kidney disease [3]. However, the putative association between uric acid in the blood and diabetes is unclear, the results are controversial, and there may be sex and race differences [4].

The uric acid (H_4UA) in the ionization form is accompanied by the tautomeric transformation keto-enol form [5, 6].



Uric acid complexes of some transition metal salts of series (3d and 5d) [7, 8], lanthanides (4f and 5f) [9], and metal ions of groups I, II, and IVa [10–13] have been prepared and characterized. The urate complexes are of interest because of their analytical and physiological applications dependent on stereochemistry [14–20]. Here we have synthesized and characterized (spectroscopic, thermal, morphological, and biological) the tellurium(IV), tantalum(V), selenium(IV), and niobium(V) metal complexes

Experimental. Pure grade chemicals throughout this study ($TeCl_4$, $TaCl_5$, $SeCl_4$, $NbCl_5$, and uric acid) were received from Sigma-Aldrich Chemical Corporation, St. Louis, Mo, USA and used without further recrystallization. For elemental analyses is used a Perkin Elmer CHN 2400; for conductance is used a Jenway 4010 conductivity meter; for FTIR spectra is used a Bruker FTIR spectrophotometer; for electronic spectra is used a UV2 Unicam UV/Vis Spectrophotometer; for magnetic moment is used a Magnetic susceptibility balance; for 1H -NMR spectra is used a Varian Mercury VX-300 NMR spectrometer, 300 MHz; for thermo gravimetric is used a TG/DTG–50H, Shimadzu thermogravimetric analyzer; for SEM is used a Quanta FEG 250 equipment; for XRD is used a X'Pert PRO PANalytical, with copper target; for TEM is used a JEOL 100s microscopy.

The metal urates $[Te(H_3UA)(H_2O)_3(Cl)] \cdot 2Cl \cdot 2H_2O$ (I), $[Ta(H_3UA)(H_2O)_2(Cl)_2] \cdot 2Cl \cdot 4H_2O$ (II), $[Se_2(H_2UA)(Cl)_4] \cdot 2Cl \cdot 4H_2O$ (III) and $[Nb_2(H_2UA)(Cl)_8] \cdot 3H_2O$ (IV) were prepared by the addition of 1 mmole of uric acid adjusted to a pH 8–9 with (0.1 M) NaOH dropwise with continuous stirring to 20 mL aqueous solution of the respective metal(IV/V) chloride ($TeCl_4$, $TaCl_5$, $SeCl_4$, and $NbCl_5$) (1 mmole). The resulting reaction mixtures of metal ions: uric acid molar ratio 1:1 or 2:1 was neutralized to a pH in the range 7–8 by a dropwise addition of 0.1 M solution of NaOH. The reaction mixtures were then heated at 80°C for about 3 h to achieve turbidity, and then left to stand at room temperature for 24 h. The formed precipitate

was filtered out, washed several times with hot water to remove the soluble cations and anions, and then dried to a constant weight under vacuum over anhydrous calcium chloride. The elemental analysis results obtained were summarized and given in Table 1.

TABLE 1. Elemental Analysis Data, Yield, and Molar Conductance of Synthesized Metal Urate Complexes

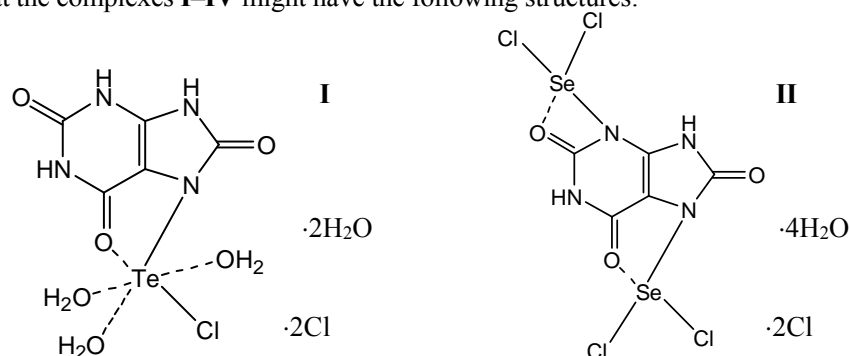
| Complexes | C, % | H, % | N, % | M, % | Yield, % | Λ , $\Omega^{-1} \cdot \text{cm}^2 \cdot \text{mol}^{-1}$ |
|-----------|------------------|----------------|------------------|------------------|----------|--|
| I | 12.18 (12.23) | 2.54 (2.67) | 11.32 (11.41) | 25.65 (25.98) | 78 | 86 |
| II | 9.94 (10.04) | 2.39 (2.53) | 9.30 (9.37) | 30.18 (30.26) | 84 | 123 |
| III | 9.78 (9.86) | 1.45 (1.66) | 9.04 (9.20) | 25.87 (25.94) | 73 | 112 |
| IV | 8.64 (8.71) | 1.10 (1.17) | 8.09 (8.12) | 26.80 (26.95) | 75 | 31 |

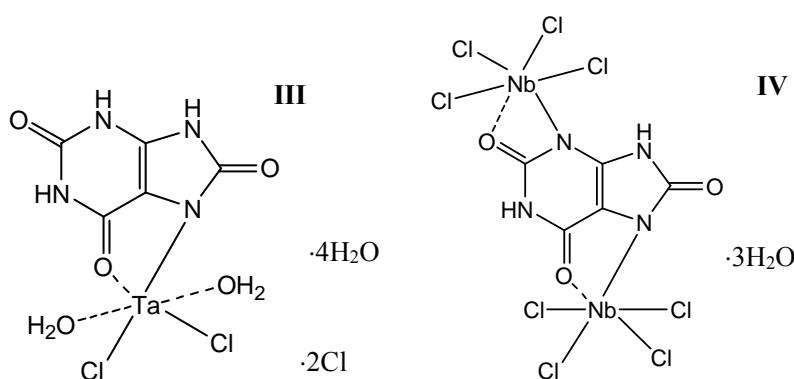
*The calculated values were shown in parenthesis.

A screening test for possible antibacterial activity was done against four bacterial strains: *Klebsiella*, *Escherichia coli*, *Staphylococcus aureus*, and *Staphylococcus epidermidis*. Using the disc diffusion method [21] to test the antimicrobial effect. Inhibition zones diameters around the disc were determined.

In vitro, the cytotoxic activity of the tested urate complexes against two human cancer cell lines (colorectal adenocarcinoma (Caco-2) and breast cancer (MCF-7)) was evaluated using the standard neutral red uptake assay [22].

Results and discussion. *Elemental and conductance analyses.* The aim of the present work was to prepare in solid-state the urates of some tetra- and pentavalent metal ions, Te^{4+} , Ta^{5+} , Se^{4+} , and Nb^{5+} to investigate the mode of interaction of uric acid with these metal ions. The reaction products were characterized using their elemental analysis, infrared spectra, and thermal analysis. In these complexes, uric acid behaves as a bidentate ligand. Urate metal complexes were synthesized with 1:1 and 2:1 molar ratio. Examination of solubility of these complexes shows that they are insoluble in most organic solvents, and slightly soluble in DMSO and DMF. The physical characteristics of these are given in Table 1. The structure of the complexes suggested from the elemental analyses agree well with their proposed formulae (Table 1). The detected values of the elemental analysis agree well with the calculated percentages of CHN data and are in good agreement with each other and prove the molecular formulas of the complexes. The observed molar conductance values of the tellurium(IV), tantalum(V), selenium(IV), and niobium(V) urate in DMSO are in the range of $31\text{--}123 \Omega^{-1} \cdot \text{cm}^2 \cdot \text{mol}^{-1}$ at room temperature. Hence, from the conductivity measurement, it is concluded that the number of chloride ions is covalently bonded to metal ions, which indicates that they act as ligands, and the others are presented as ionic outside the coordination sphere. Based on the metal-ligand ratio calculated by the analytical data and the nature of the electrolytes given by the conductance measurements, compositions were assigned for the prepared complexes. From the elemental analysis and conductance analysis, it is predicted that the complexes I–IV might have the following structures:





FTIR analysis. The infrared assignments of the distinguished vibration bands of H₄UA ligand and the synthesized urate complexes **I–IV** are tabulated in Table 2. The infrared spectra of urate complexes **I–IV** were scanned within the region 4000–400 cm⁻¹ (Fig. 1). In the urate complexes, the new absorption broadband lying in the region 3390–3470 cm⁻¹ is attributed to $\nu(\text{O–H})$ of coordinated and uncoordinated water molecules [23]. Regarding the stretching vibration band at 3015 cm⁻¹ placed in the IR spectrum of H₄UA, this is attributed to $\nu(\text{N–H})$; this band is absent or shifted to lower wavenumbers after binding of the uric acid ligand towards respected metal ions [17, 19]. It has been suggested that the involvement in the coordination process, while those bands are below the 2700 cm⁻¹ region, is due to the hydrogen bonds $\nu(\text{NH}\dots\text{O})$ [17–20].

TABLE 2. Infrared Assignments of Urate Complexes **I–IV**

| Compounds | Assignments | | | | | | | | | |
|-------------------|------------------|------------------|---------------------|---------------------|-------------------|-------------------|-------------------|-------------------|-------------------|-------------------|
| | $\nu(\text{OH})$ | $\nu(\text{NH})$ | $\nu(\text{C=O}_p)$ | $\nu(\text{C=O}_i)$ | $\nu(\text{C=C})$ | $\nu(\text{C=N})$ | $\nu(\text{C–N})$ | $\nu(\text{C–O})$ | $\nu(\text{M–O})$ | $\nu(\text{M–N})$ |
| H ₄ UA | – | 3015 | 1701 1671 | 1655 | 1587 | 1434 | 1326 | 1122 | – | – |
| I | 3467 | – | 1686 | – | 1443 | 1384 | 1287 | 1013 | 595 517 | 478 |
| II | 3434 | 2969 | 1643 | – | 1460 | – | 1207 | 1079 | 628 | 559 |
| III | 3461 | – | 1686 | – | 1461 | – | 1193 | 1023 | 601 | 502 |
| IV | 3392 | 2983 | 1643 | – | 1447 | – | 1207 | 1079 | 628 | 559 |

Free H₄UA has characteristic bands at 1701, 1671, and 1655 cm⁻¹ due to $\nu(\text{C=O})$ stretching vibration bands of the carbonyl groups [18, 19], and those bands at 1587, 1434, 1326, and 1122 cm⁻¹ are assigned to $\nu(\text{C=C})$, $\nu(\text{C=N})$, $\nu(\text{C–N})$, and $\nu(\text{C–O})$, respectively. This is strong evidence that the structure of the H₄UA ligand is keto-enol tautomerized before complexation with metal ions [20]. The stretching vibration bands at 1701 and 1671 cm⁻¹ is assigned to the carbonyl of the pyrimidine ring, and the other band at 1655 cm⁻¹ is due to the carbonyl of the imidazole ring [24]. Concerning the synthesized urate complexes **I–IV**, the $\nu(\text{C=O})$ bands are shifted to lower wavenumber or absent compared with free H₄UA ligand; this indicates that at least one of the carbonyl groups is coordinated towards metal ions. This observation suggests that one of the two carbonyl groups in the pyrimidine ring is involved in the coordination with metal ions leaving the other group unaffected by this coordination. This suggestion could be supported by observing an infrared band 1013–1079 cm⁻¹ in the spectra of urate complexes with the shifter to lower wavenumbers. This band is observed in the spectrum of free H₄UA at 1122 cm⁻¹ and might be attributed to the $\nu(\text{C–O})$ stretching vibration [23]. All urate complexes show an infrared absorption band within the 850–900 cm⁻¹ region attributed to rocking bending motion $\delta_r(\text{H}_2\text{O})$ of the coordinated water. New bands within the 628–478 cm⁻¹ region with weak-to-medium weak intensities are due to the stretching vibrations of $\nu(\text{M–N})$ and $\nu(\text{M–O})$ bands [23]. Accordingly, uric acid in these complexes behaves as a bidentate ligand in the anionic form and coordinates to metal ions through the pyrimidine oxygen C(6)=O group and N(7), as well as N(3) of the imidazole ring.

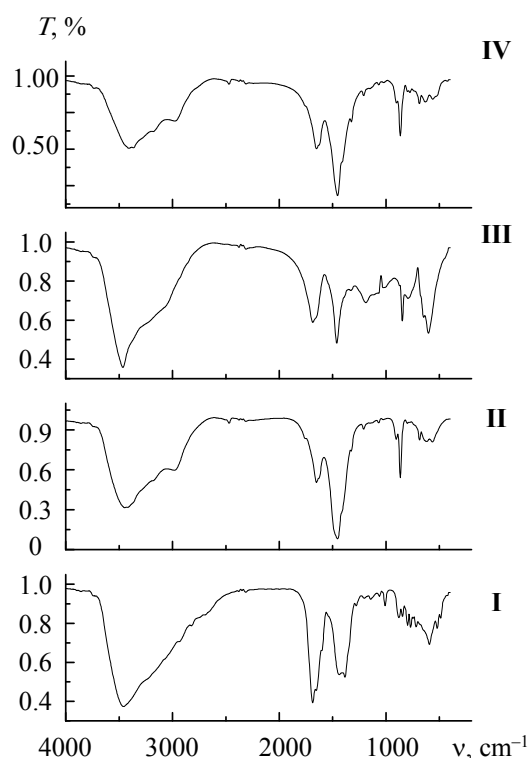


Fig. 1. FTIR spectra of urate complexes **I**, **II**, **III**, and **IV**.

Electronic spectra. The UV-Vis spectrum of H_4UA free ligand has a maximum peak at 292 nm [5] that can be assigned to $n-\pi^*$ transition concerning the carbonyl groups; after ionization, it will be shifted to longer wavenumber [5, 6]. This observation confirmed that the keto form is the most stable form. After complexation, the distinguish peak of H_4UA at 290 nm is shifted to a lower wavelength at 265–274 nm, due to the sharing of the carbonyl group in coordination toward metal ions. The new peak at 372–392 nm might be due to either a metal-to-ligand or ligand-to-metal electron transfer in the synthesized urate complexes **I–IV** [25].

1H NMR spectra. The 1H -NMR study was carried out in DMSO for urate complexes to know which $-NH$ group proton among the four in H_4UA [N(1)-H, N(3)-H, N(7)-H, or N(9)-H] has been deprotonated during complexation (Table 3). After the coordination of Te(IV), Ta(V), Se(IV), and Nb(V) metal ions, the protons of H_4UA undergo a change in their chemical shift values, typically upfield due to increased conjugation. It was also observed that the signals in the H_4UA spectrum appear at 10 ppm for N(1)-H group proton, N(3)-H, N(7)-H, and N(9)-H at 6 ppm values, respectively, whereas the urate complexes **I–IV** show the signal at 5.407–5.446 ppm for only one N-H imidazole proton with an upfield shift, but those three signals were absent due to complexation because it changes the environment of protons. A sharp signal appeared at 3.334–3.379 ppm, which represents the presence of water molecules in the complex structure. The 1H NMR spectra of the solid urate complexes indicate that H_4UA in these complexes behaves as a bidentate ligand through the deprotonated N-7 with the imidazole ring and O-6 within the pyrimidine ring, whereas in the case of the binuclear complexes of selenium(IV) and niobium(V) the coordination take place through N-7 and O-6 as well as N-3 and O-2.

TABLE 3. 1H -NMR Proton Signals of Urate Complexes

| Assignments | H_4UA | I | II | III | IV |
|-------------|---------|----------|-----------|------------|-----------|
| 1H, N(1)-H | 10 | – | – | – | – |
| 1H, N(3)-H | 6 | | | | |
| 1H, N(7)-H | 6 | 5.435 | 5.407 | 5.446 | 5.420 |
| 1H, N(9)-H | 6 | | | | |
| 2H, H_2O | – | 3.343 | 3.372 | 3.379 | 3.334 |

Thermal study. The thermograms (TGA and DrTGA) of tellurium, tantalum, selenium, and niobium urate complexes **I–IV** were scanned under an N_2 atmosphere (Fig. 2). Thermal decomposition of these complexes passes through three-to-five stages. The first step of thermal cracking takes place within the temperature range of 30–250°C due to the liberation of uncoordinated and coordinated water molecules. The mass losses regarding this step are assigned to the loss of five, six, four, and three water molecules for the complexes **I–IV**. The endothermic dehydration step for the urate complexes **I–IV** occurs in one-to-two steps at DrTGA = 105, 110, 118, and 120°C, respectively. These results confirm the presence of water molecules inside and/or outside the coordination sphere. The second-to-five stages of thermal decomposition take place within a temperature of range 150–800°C and can be assigned to the decomposition of urate moieties to the corresponding metal oxychloride as $TeOCl_2$, $TaOCl_3$, and $SeOCl_2$, while the complex **IV** has a niobium metal as a residue. The detected weight losses (57.49, 51.15, 59.43, and 72.50%) associated with this stage agree well with the calculated weight losses (56.32, 49.27, 59.78, and 73.05%) due to the loss of the urate molecules and some of the chlorine atoms at DrTGA = (290, 503, 562, and 633°C), (380 and 655°C), (376, 555, and 658°C), and (286 and 420°C), for the urate complexes **I–IV**, respectively.

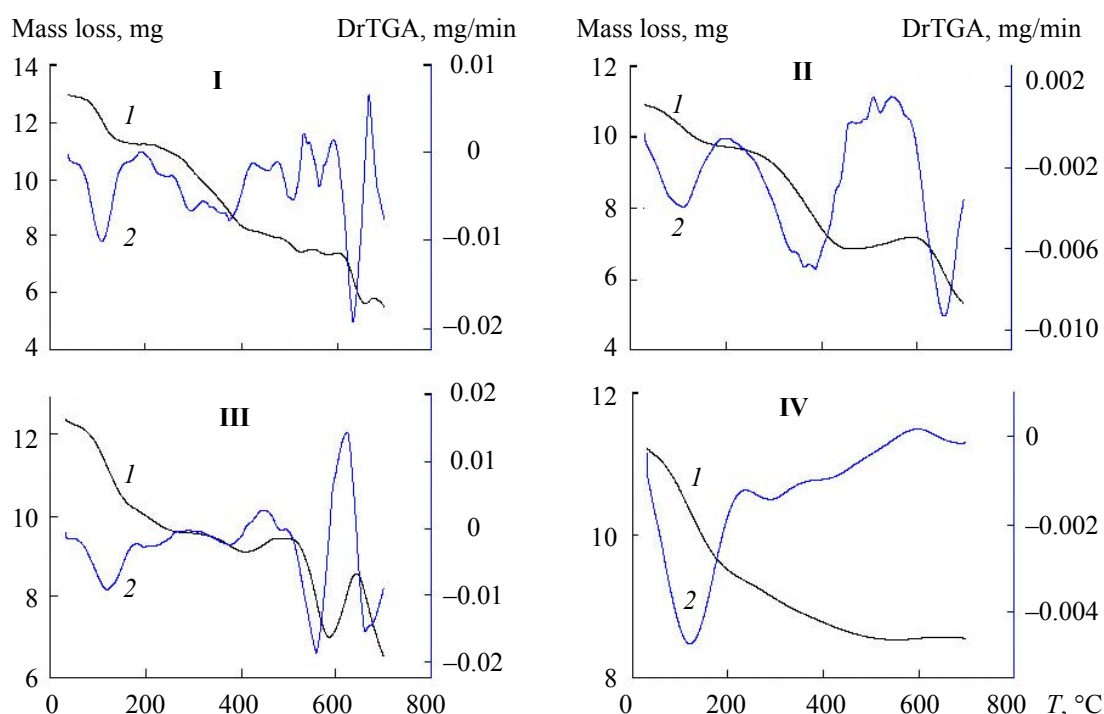


Fig. 2. TGA (1) and DrTGA (2) curves of urate complexes **I–IV**.

Surface and particle sized analysis. To obtain good information on the surface morphology and the particle size of the urate complexes **I–IV**, SEM analysis was performed. The SEM micrographs (Fig. 3) at 20,000× magnification value show that the solid products have a compacted plates-shaped structure with well-defined particles. The increase in the magnification did not allow for better differentiation of the particles. The formation of tellurium(IV), tantalum(V), selenium(IV), and niobium(V) urate complexes results in aggregates comprising very tiny three-dimensional disordered primary nanoparticles. The particles exhibit irregular forms, and their size is widely distributed between 30 nm and 5 μ m. XRD patterns are the most useful technique for the identification of crystalline structure, and was employed to investigate the crystallinity and purity of the solid products of the urate coordination compounds. The XRD pattern of the solid urate complexes (Fig. 4) shows the presence of the characteristic peaks for metal ions and urate molecules in the range of $2\theta = 4\text{--}90^\circ$. In Fig. 4, the 2θ values with maximum intensity of the peaks for urate complexes **I–IV** are observed at $2\theta = (10.48, 14.14, 19.78, 29.07, 31.90, 33.86, 38.09, \text{ and } 45.72^\circ)$, $(11.87, 16.95, 32.47, 33.58, 36.41, 38.09, 40.36, 45.44, 51.06, 55, 57.27, \text{ and } 75.32^\circ)$, $(18.65, 29.07, 31.90, 34.15, 36.99, 40.36, 45.72, 58.12, \text{ and } 75.60^\circ)$, and $(16.95, 32.47, 33.86, 37.81, 45.15, \text{ and } 57.27^\circ)$, which correspond to metal

ion and urate ligand. The crystallite size of the solid complexes **I–IV** was calculated using the Scherrer formula [26]. The estimated crystallite size of the analyzed solid products from the highest diffraction peak at 29.07, 75.32, 31.90, and 32.47°, respectively for urate complexes **I–IV**, is approximately within 12–30 nm. Figure 5 shows that the TEM images of the prepared **III** and **IV** nanoparticles are approximately spherical, with the diameter varying between 10 and 20 nm and 15 and 48 nm, respectively.

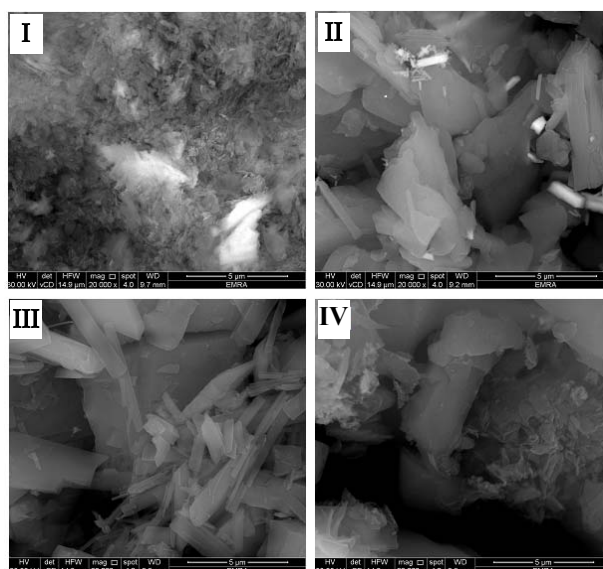


Fig. 3. SEM images of **I–IV** urate complexes.

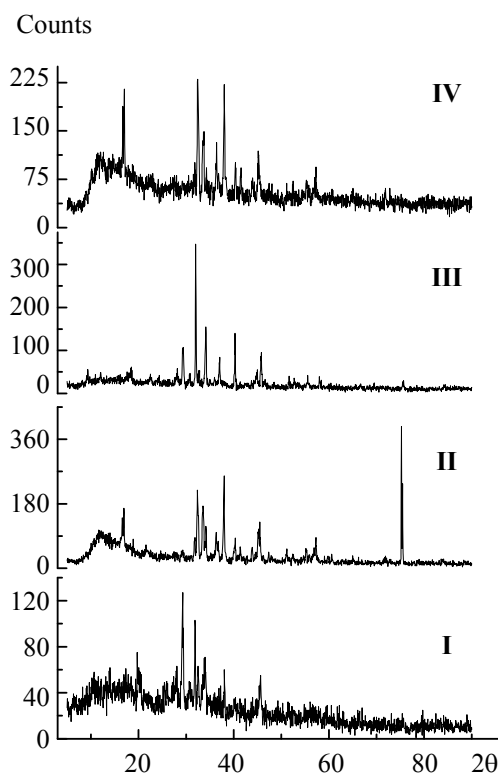


Fig. 4. XRD pattern of **I–IV** urate complexes.

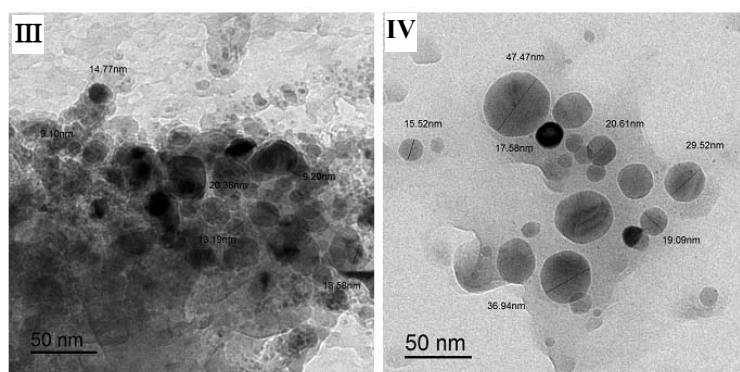


Fig. 5. TEM images of **III** and **IV** urate complexes.

Biological study. A screening test for a possible antibacterial activity for the four synthesized complexes was done using the disc diffusion method (Table 4). We detected no antibacterial activity regarding the *Staphylococcus aureus* and *Staphylococcus epidermidis* microorganisms against all tested urate complexes, but there was a slight activity for all complexes against *Klebsiella*. Also, the complex **IV** shows some efficiency against *Escherichia coli*.

TABLE 4. Inhibition Zone Diameter of Urate Complexes

| Sample | | Inhibition zone diameter (mm/mg sample) | | | |
|---------------|-------------|---|---|---|--|
| | | <i>Klebsiella</i> (-ve) | <i>Escherichia</i> <i>Coli</i> (-ve) | <i>Staphylococcus</i> <i>Epidermidis</i> (+ve) | <i>Staphylococcus</i> <i>Aureus</i> (+ve) |
| Control: DMSO | | 0.2 | 0.0 | 0.0 | 0.0 |
| Standard | Ceftriaxone | 0.0 | 0.0 | 1.6 | 1.9 |
| | Gentamycin | 0.3 | 0.0 | 1.8 | 1.5 |
| S 31 | | 0.4 | 0.0 | 0.0 | 0.0 |
| S 32 | | 0.3 | 0.0 | 0.0 | 0.0 |
| S 33 | | 0.4 | 0.0 | 0.0 | 0.0 |
| S 34 | | 0.2 | 0.3 | 0.0 | 0.0 |

To test the anticancer effect of the synthesized four urate complexes, two human cancer cell lines were selected: colorectal adenocarcinoma cell line (Caco-2) and breast cancer cell line (MCF-7). The results revealed no anticancer effect for three of the complexes **II**, **III** and **IV**. Using the neutral red uptake assay, the cell viability percentages after treatment were high in both cell lines (>100 $\mu\text{g/ml}$). The complex **I** was unable to completely dissolve in the solvent.

Conclusions. We would like to point out that in this research paper, four metal salts (tellurium, tantalum, selenium, and niobium) have been worked on, and they are novel in terms of their binding of uric acid. We describe the association between those metals and uric acid in 1:1 and 1:2 ratios, and the compounds formed. The formed compounds were examined using several analyses, indicating the nature of bonding as that Te^{4+} and Ta^{5+} mononuclear complexes have a six-coordinate geometry through a carbonyl oxygen atom of $\text{C}(6)=\text{O}$ group and the deprotonated $\text{N}(7)$, but both Se^{4+} and Nb^{5+} binuclear complexes have a binding with respected metal ions through $\text{C}(6)=\text{O}$ group and the deprotonated $\text{N}(7)$ beside $\text{C}(2)=\text{O}$ group and the deprotonated $\text{N}(3)$. We also suggest that the selenium ion is four-coordinated. The analyzes that were used in this study are consistent with what was used in the previous research, except for the analyzes that were added in this study, which are the studies of the nature of surfaces of solid compounds formed, such as SEM, TEM, and XRD. These surface characterizations indicate that the particle size of the synthesized complexes is within 10–50 nm.

Acknowledgments. This work was funded by the Deanship of Scientific Research at Princess Nourah bint Abdulrahman University, through the Research Groups Program (Grant No. RGP-1440-0001) (2).

REFERENCES

1. C. Remedios, M. Shah, A. G. Bhasker, M. Lakdawala, *Obes. Surg.*, **22**, 945 (2012).
2. G. Glantzounis, E. Tsimoyiannis, A. Kappas, D. Galaris, *Curr. Pharm. Des.*, **11**, 4145 (2005).
3. N. Ali, S. Rahman, S. Islam, T. Haque, N. H. Molla, A. H. Sumon, R. R. Kathak, M. Asaduzzaman, F. Islam, N. C. Mohanto, M. A. Hasnat, S. M. Nurunnabi, S. Ahmed, *BMC Cardiovasc. Disord.*, **19**, 42 (2019).
4. T. Haque, S. Rahman, S. Islam, N. H. Molla, N. Ali, *Diabetol. Metab. Syndr.*, **11**, No. 49, 1 (2019).
5. G. D. Christain, *Analytical Chemistry*, 3rd ed., Wiley, New York, 528 (1980).
6. M. Kamiyal, N. Haba, Y. Akahor, *Chem. Pharm. Bull.*, **21**, 1474 (1973).
7. C. M. Mikulski, M. Holman, G. Tener, T. Dobsoti, S. Eana, W. Weish, *Am. Chem. Soc.*, **73**, 202 (1991).
8. F. Karl, U. Gertrud, T. H. Charlottenubrg, *Chem. Abstr.*, **14**, 1333j (1920).
9. G. Kallistratos, A. Pfauu, *Chem. Abstr.*, **71**, 87247y (1970).
10. W. Dosch, A. Matxke, *Fortschr. Urol. Nephrol.*, **22**, 279 (1984).
11. D. Erich, J. Geoffrey, B. K. Zlatan, *J. Inorg. Biochem.*, **26**, 1 (1986).
12. P. Carmona, *J. Solid State Chem.*, **55**, 292 (1984).
13. A. Martini, *Pubs. Inst. Invest. Microqum. Univnacl. Litoral.*, **5**, 35 (1941).
14. S. Muraoka, M. Sugiyama, H. Yamasaki, *Chem. Abstr.*, **62**, 13443 (1965).
15. M. J. Harris, A. Herp, W. Pigman, *J. Am. Chem. Soc.*, **94**, 7570 (1972).
16. S. F. Wong, B. Halliwell, R. Rochmond, W. R. Showroneck, *J. Inorg. Biochem.*, **14**, 127 (1981).
17. V. V. Ramana, V. J. Thyagaraju, K. S. Sastry, *J. Inorg. Biochem.*, **48**, 85 (1992).
18. W. Brzyska, M. Sikorska, *Pol. J. Chem.*, **66**, 253, 403 (1992).
19. M. M. Moawad, *J. Coord. Chem.*, **55**, No. 1, 61 (2002).
20. M. S. Masoud, A. E. Ali, M. A. Shaker, G. S. Elasala, *Spectrochim. Acta A*, **90**, 93 (2012).
21. A.W. Bauer, W. A. Kirby, C. Sherris, M. Turck, *Am. J. Clin. Pathol.*, **45**, 493 (1996).
22. G. Repetto, A. del Peso, J. L. Zurita, *Neutral Red Uptake Assay for the Estimation of Cell Viability/Cytotoxicity*, Nature Protocols (2008).
23. K. Nakamoto, *Infrared and Raman Spectra of Inorganic and Coordination Compounds*, Wiley, New York (1986).
24. H. Biltz, *Chem. Ber.*, **69B**, 2750 (1936).
25. R. M. Silverstein, F. X. Webster, D. J. Kiemle, *Spectroscopic Identification of Organic Compounds* (1981).
26. B. D. Cullity, S. R. Stock, *Elements of X-ray Diffraction*, Prentice Hall, New York (2001).